Journal of Power Sources 196 (2011) 7411–7419

Contents lists available at ScienceDirect

Journal of Power Sources

journal homepage: www.elsevier.com/locate/jpowsour

From microstructure to the development of water and major reaction sites inside the catalyst layer of the cathode of a proton exchange membrane fuel cell

Ming-San Lee*, T.H. Chen, W.S. Lee, B.S. Lin, B.Y. Lau, P.F. Tsai, G.C. Wang

Department of Mechanical Engineering, National Sun Yat-Sen University, Kaohsiung, Taiwan 80424, Republic of China

ARTICLE INFO

Article history:
Received 13 January 2011
Received in revised form 10 April 2011
Accepted 13 April 2011
Available online 20 April 2011

Keywords:
Microstructure
Major reaction sites
Water surface
Cathode
Proton exchange membrane fuel cell

ABSTRACT

Microstructures of various sizes and shapes are fabricated on the surface of the catalyst layer (CL) of the cathode of a PEMFC, adjacent to the micro porous layer (MPL). Three major experimental results are: (1) performance is improved by up to 60% and the percentage of the increase is the same as that of the increase in interface area of CL and MPL; (2) the cell suffers no significant performance loss when Pt loading of the cathode is reduced from 1 to 0.25 mg cm^{-2} and; (3) transient responses in periodical linear sweep tests show an obvious performance "jump" for all the cathodes with microstructures when approaching steady state, but none for others. Based on observations, a proposal related to the development of water and, consequently, the major reaction sites in the CL is made: there is a general water "surface" inside the CL. Major electrochemical reactions occur above (on the MPL side) of this surface and within a limited height. The surface will "move" from the membrane toward the MPL as more water is produced. The vapor generation rate (current load) relative to the removal rate of the rest of the cell components will determine the steady state position of this water surface.

1. Introduction

The conventional structure of the catalyst layer of an electrode is a thin flat layer with uniform composition. Recently, research has emerged exploring the possibility of enhancing catalyst performance through structural modification.

1.1. Various structural modifications to the catalyst layer

Lee et al. [1] proposed building a microstructure on the surface of the catalyst layer, adjacent to MPL, to enhance the catalyst's performance, and showed that the area of the interface of CL and MPL correlates positively with cell performance. Other studies have focused on the catalyst layer's other surface, i.e., the interface of the CL and the electrolyte membrane. Cho et al. [2] bombarded the surface of a Nafion 115 membrane with an Ar^+ ion beam to roughen its surface and thus enlarge the effective area of the interface. Prasanna et al. [3] extended this work showing significant results in Pt loading with a membrane treated by Ar^+ ion beam bombardment. Hakan Yildirim et al. [4] and Zhang et al. [5] respectively applied hot embossing and nanoimprint techniques to generate micro-patterns on the Nafion membrane of a DMFC to enlarge the catalyst surface area without increasing the geometric surface area of the MEA.

Another approach for structural modification is the multi-catalyst layer technique which divides the conventional single uniform catalyst layer into 2–4 layers, each with different Pt loadings in different Pt/C wt.% and, sometimes, with different Nafion contents. Taylor et al. [6] used inkjet printing techniques to produce a catalyst layer of a graded structure with 3 layers of 10, 20, and 50 wt.% of Pt, with the layer with the highest concentration located closest to the electrolyte. Su et al. [7] developed an ultra-low Pt loading MEA with a double catalyst layer structure. The result had an 80% (made with 40 wt.% Pt/C) and 20% (made with 10 wt.% Pt/C) Pt distribution in the inner (membrane side) and outer (GDL side) layer, respectively, for both cathode and anode. The Nafion contents were also different, with 33% and 20%, respectively, for the inner and the outer layer. The results show performance improvement in the high current region. Srinivasarao et al. [8] conducted numerical analysis on the performance of a PEMFC cathode with multiple catalyst layers. Yoon et al. [9] and Kim et al. [10] only changed the Nafion content inside the catalyst layer from a uniform composition into two different compositions, with the inner layer having a higher content. The results show that cell performance improved in the high current density region.

For these structural modifications to be effective, as many "additional" triple phase boundary (TPB) sites as possible should be created inside the catalyst layer. A three-dimensional porous structure with many nano-sized Pt particles covering the inner surface of the pores is designed to facilitate both the gaseous phase (oxygen) and the solid phase (Pt catalyst). But, where is the liquid phase

* Corresponding author. Tel.: +886 7 525200x4225; fax: +886 7 5254299.
E-mail address: mslee@mail.nsysu.edu.tw (M.-S. Lee).

0378-7753/$ – see front matter © 2011 Elsevier B.V. All rights reserved.
doi:10.1016/j.jpowsour.2011.04.022

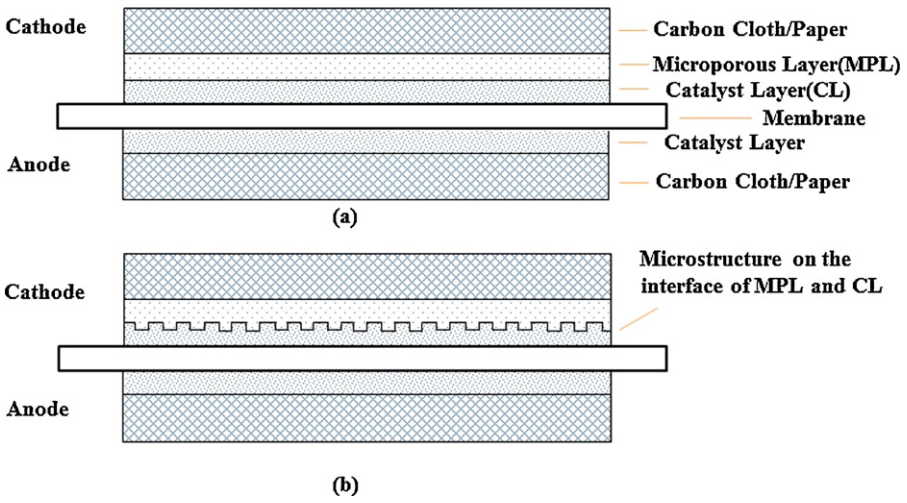

Fig. 1. Schematic illustration of the structure of MEAs: (a) conventional with flat CL and MPL, and (b) the hydrophobic micro pillar structure (HMPS) on the interface.

(water)? Protons have to stay in the water and move through water molecules. A "continuous" water channel must be established from the membrane to the desired reaction location. Unfortunately, water obstructs the movement of gaseous oxygen. Obviously, the distribution of water holds the key to determining where the reaction should take place and which modification is valid.

1.2. No tool available to monitor the distribution of water inside catalyst layer pores

Bazylak [11] reviewed more than 89 papers on water related topics in PEMFC, listing and discussing both the advantages and disadvantages of various observation methods including nuclear magnetic resonance (NMR) imaging, also known as magnetic resonance imaging (MRI) [12,13], neutron imaging [12,14], synchrotron X-ray [15,16], micro tomography [17], optical photography [18,19], and fluorescence microscopy [20,21]. Due to their restricted resolution and response time, these techniques can only spot larger water droplet gatherings [22]. They are unable to "see" the condition of liquid water inside the nano-pores in the catalyst layer, let alone determine where a particular water molecule is generated and which path it will take leaving the cathode.

Zhang et al. [23] published one of the few studies to focus on the condition of water inside the catalyst layer. They removed a small piece of GDL to observe the catalyst layer directly. They conclude that larger pores will fill with liquid water first and thus will be unable to participate further in the reaction. Thus, the only "reacting" pores are the smaller ones that, the authors believe, require a higher vapour pressure to remain active. If this is the case, water should leave the catalyst layer in the form of vapour because water-blocked pores will unable to generate "new" water to push the "old" water out. Studies by Hartnig et al. [15] and Weber and Hickner [24] also suggest that vapour is the major form by which water leaves the CL.

Litster et al. [21] applied fluorescence microscopy to observe the movement and distribution of water inside GDL. Rather than use the well-known upside-down tree model, also known as a converging capillary tree [25], they proposed another model for the transport of water called fingering and channelling. These water development models have difficulty explaining our experimental observations of "moving" major reaction sites (MRS) because a fixed "irrigation" system usually implies that the reaction sites are fixed as well.

This paper will illustrate the design and fabrication of the microstructure and then explain how its effectiveness can be related to the distribution of water and, consequently, the reaction sites inside the catalyst layer.

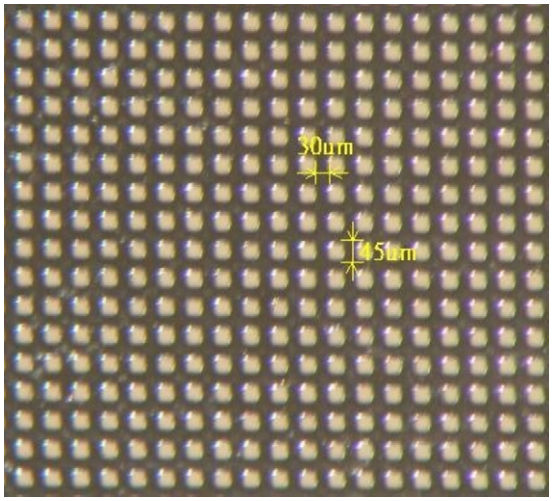

Fig. 2. Metal mould with mesh of 45 μm × 45 μm and interstices of 30 μm to produce a hydrophobic micro pillar structure (HMPS) using imprint technology.

2. Experimental

2.1. Design

The idea of having a microstructure on the surface of the catalyst layer, next to MPL, to enhance catalyst performance was first raised by Lee et al. [1]. Fig. 1 compares the structure of the new concept to that of the conventional design. The microstructure was initially built using a metal net as a mask and the fabrication process was tedious because the net was easily clogged with carbon powder and needed to be rinsed constantly. In this study, a metal mould with dimensions shown in Fig. 2 is made and identical hydrophobic micro pillar structures (HMPS) are created through imprinting.

Theoretically, a multilayer pyramidal microstructure can produce an increase in interface area in excess of 100%. Fig. 3 shows a mould of a 2-layer pyramidal microstructure. The rounded corners are due to inaccuracies in manufacturing that limited the increase to about 60%. However, the method provides other advantages such as easy mould release, simple fabrication process, and lower Pt loading.

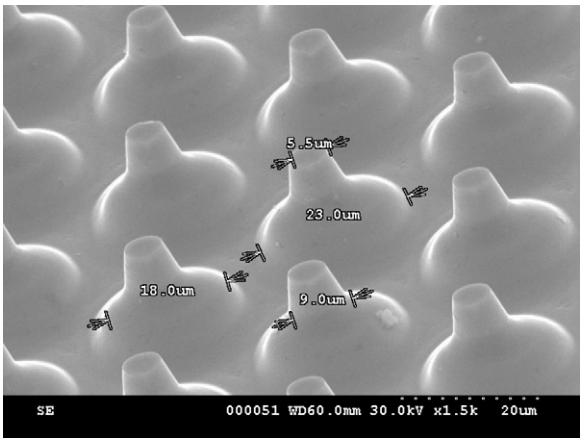

Fig. 3. Metal mould to produce the 2-layer pyramidal microstructure.

Although the roller imprint technique may be used to fabricate microstructures for the production of large-area electrodes, mould preparation is still quite expensive. An easier and faster way is to spray larger carbon spheres onto the interface to function as microstructures as illustrated in Fig. 4. Of course, the two cases are different in that (1) fuel can diffuse "through" a microstructure whereas fuel can only flow "around" a larger carbon sphere, and (2) the exact increase of the interface area of the spheres is difficult to calculate and, thus, will not elaborated further in this design.

2.2. Fabrication

Fig. 5 illustrates the fabrication process, which can be divided into four major steps as follows:

1. Create the MPL by spraying about 1 mg cm^{-2} of a mixture of carbon powder (E-Tek, Vulcan XC-72) and PTFE (DuPont Fluoroproducts, Teflon® PTFE 30 Dispersion), with a weight ratio of 1:1 onto a piece of carbon cloth (E-Tek, carbon cloth Designation A, 20 wt.% wet proofing). Heating the cloth for 2 h at 340 °C.
2. Create microstructures on the MPL by pressing the mould against it.
3. Remove the metal mould.

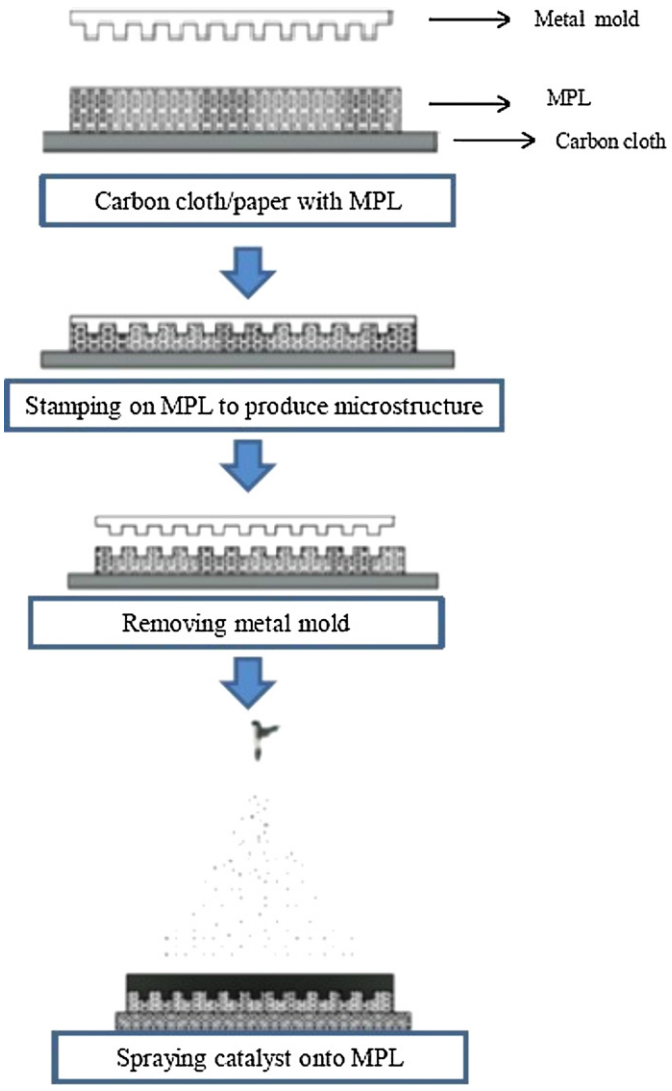

Fig. 5. Schematic illustration of a microstructure fabricated with nano-imprint technology.

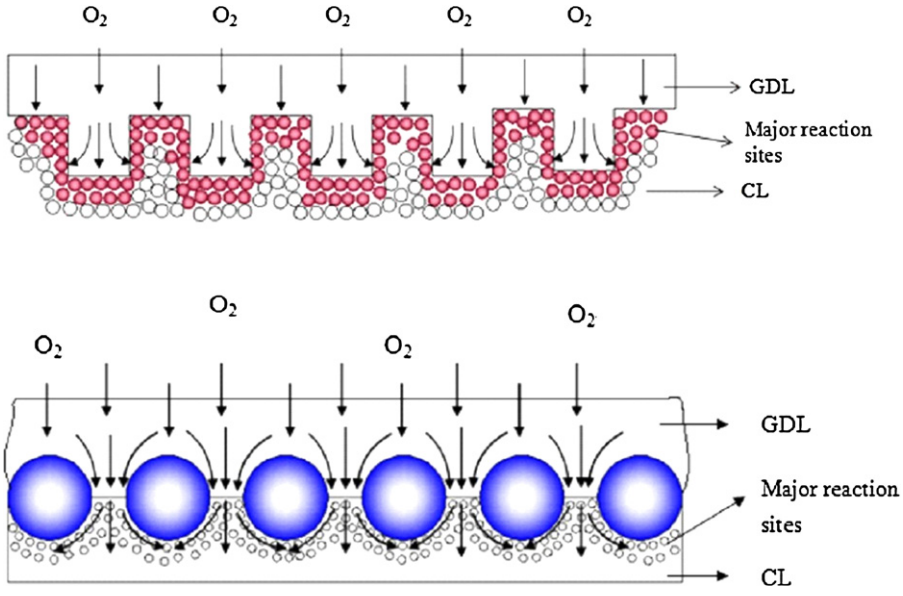

Fig. 4. Schematic illustration of the use of large carbon spheres to function as a microstructure in the production of large-area electrodes.

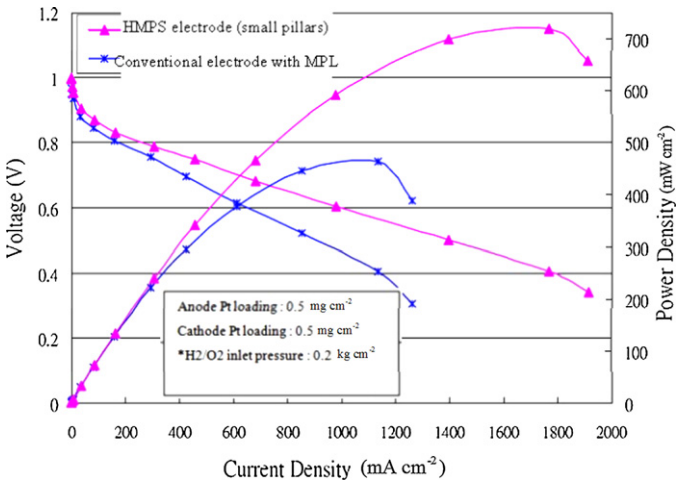

Fig. 6. Performance comparison between the small hydrophobic micro pillar structure (45 μm × 45 μm × 20 μm) and the conventional structure (flat MPL and catalyst layer).

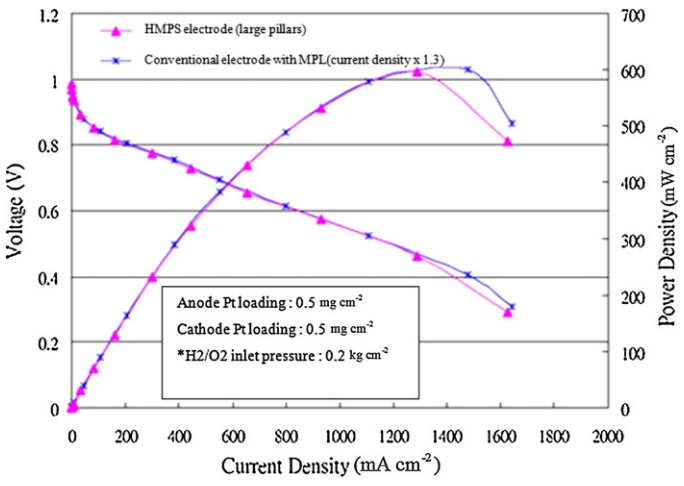

Fig. 7. Performance comparison between the large hydrophobic micro pillar structure (150 μm × 150 μm × 20 μm) and the conventional structure (current density × 1.3).

4. Spray the catalyst onto the surface with the microstructure to reach the desired Pt loading. This completes the cathode manufacturing.

2.3. Experimental setup

Since this study is focused on the performance of a specially designed cathode, a conventional anode structure (Fig. 1) is used for all experiments. The catalyst used was 60 wt.% Pt on Vulcan XC-72 (E-Tek) with a loading of 0.5 mg cm^{-2} for both the anode and the cathode. Nafion 212 was prepared through standard procedures to serve as the proton exchange membrane. The MEA was fabricated by hot pressing at 130 °C with 10 MPa for 90 s. Graphite plates with serpentine flow channels were used to construct the test cell. Hydrogen and oxygen were supplied at 0.2 kg cm^{-2} without circulation or humidification. The cell initially operated at room temperature (25 °C) but reached a steady-state value of about 55–60 °C from the heat generated in the operation. The water produced in the reaction was passively collected at the bottom of the test cell by gravity. Unless otherwise specified, all measurements were taken after the water appeared in the collecting bottle and the cell was running at steady state.

To evaluate the performance of the electrode with microstructure, a conventional electrode with a flat catalyst layer and MPL (Fig. 1(a)) was fabricated and tested in advance.

3. Results and discussion

3.1. The increase in the interface area corresponds to the increase in performance

At first, smaller micro pillars with dimensions 45 μm × 45 μm × 20 μm ($L \times W \times H$) are fabricated using imprint technology. With the distance between pillars set to 30 μm, the number of pillars per square centimetre reaches 17,700, thus creating a 60% increase in interface area over conventional MEA. In addition, the resulting electrode exhibits an approximately 60% increase in performance across the entire current spectrum compared to the conventional electrode (Fig. 6). Next, the dimensions of the micro pillars are enlarged to 150 μm × 150 μm × 20 μm ($L \times W \times H$) and set 50 μm apart so that the number of pillars per square centimetre is reduced to 2500, thus creating a 30% increase in interface area. Fig. 7 shows this electrode exhibits a 30% performance increase compared with that of the conventional electrode. The consistency of the area:performance increase ratio emphasizes the correlativity between area and performance, with the two curves nearly coincidental. A third experiment reduces the height of the smaller pillar to 10 μm so that the interface area is increased by only 30%. Fig. 8 compares the performance of this electrode to that of the larger pillars: both undergo the same increase in interface area and, again, the two curves are very close. Fig. 9 shows a performance comparison between the 2-layer pyramidal microstructure, arranged and with dimensions illustrated in Fig. 3, and the conventional structured electrode. Performance is improved by 58%, which also coincides with the increase in interface area. Once more, the two curves coincide across the entire current spectrum.

Microstructures of various dimensions, quantities, heights, shapes and designs were fabricated on the surface of the catalyst layer, adjacent to MPL. These microstructures make various contributions to the overall increase in the interface area between the catalyst layer and MPL, and produced an equal increase in performance across the entire current spectrum. The close correlativity between the two indicates that, at steady state, the major reaction sites are close to the microstructures. Based on this observation, Pt loading of the cathode was reduced from 1 to 0.5 mg cm^{-2}, and then

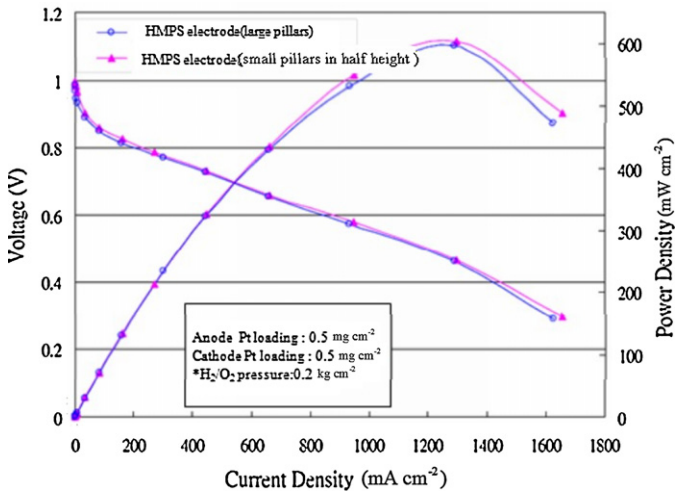

Fig. 8. Performance comparison between the large hydrophobic micro pillar structure (150 μm × 150 μm × 20 μm) and the small micro pillar in half height (45 μm × 45 μm × 10 μm).

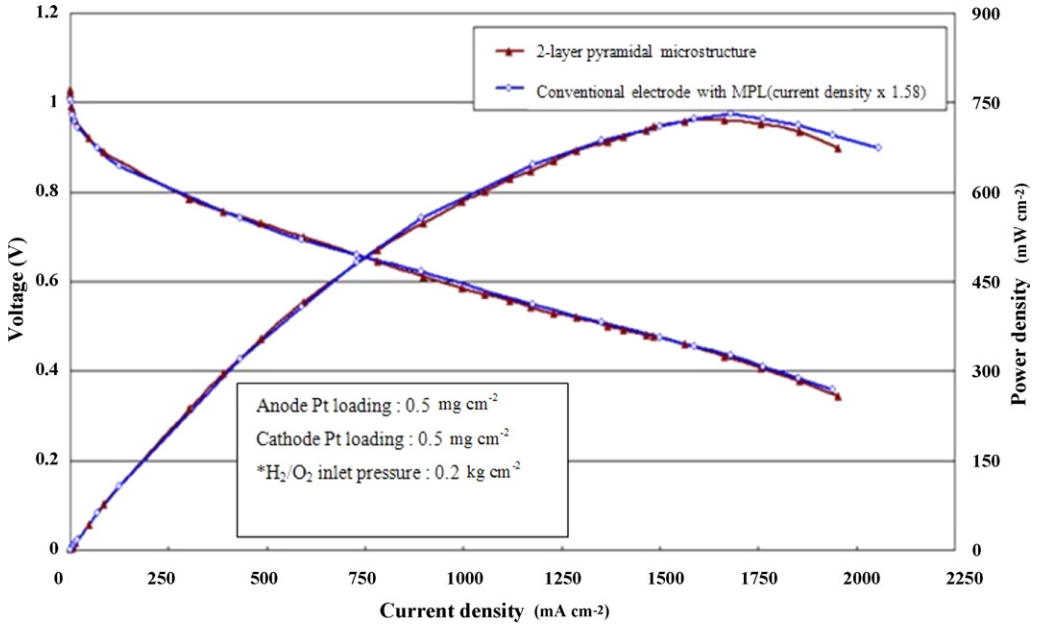

Fig. 9. Performance comparison between 2-layer pyramidal microstructure and the conventional structure (current density × 1.58).

further reduced to 0.25 mg cm^{-2} without the cell suffering any significant performance loss, as shown in Fig. 10. This indicates that, at least at steady state, not all Pt were involved in the reaction. The major reaction sites all lie away from the membrane, and it is believed this is due to the development of water produced inside the cathode.

3.2. Performance "jumps" when approaching steady state in periodic linear sweep tests

We proceeded with another experiment called the periodic linear sweep test, designed by Hao et al. [26], in which the performance of an MEA is tested in many "cycles". A "cycle" begins with a small output current and gradually increases the current stepwise to its maximum, and then reverses the process back to the small current, with continuous recording of corresponding output voltages along the way. The test is done continuously in cycles until it reaches a steady state.

To establish a "similar" state of hydration, MEAs under testing were slowly dried by passing through a small amount of gas while measuring their impedances at 1000 Hz. Fig. 11 represents a typical response, i.e., a sharp rise is preceded by a flat portion. The flat portion represents that, at the beginning of the drying process, the water lost through evaporation is in the interstices of GDL or catalyst layer. The drying begins from the outside component (GDL) and gradually moves inside (to the membrane). By the time the membrane begins to lose water, the impedance increases sharply and the drying process should be terminated. A fixed value of impedance is chosen as the terminating condition. This does not necessarily represent the same state of hydration, but merely gives an indication

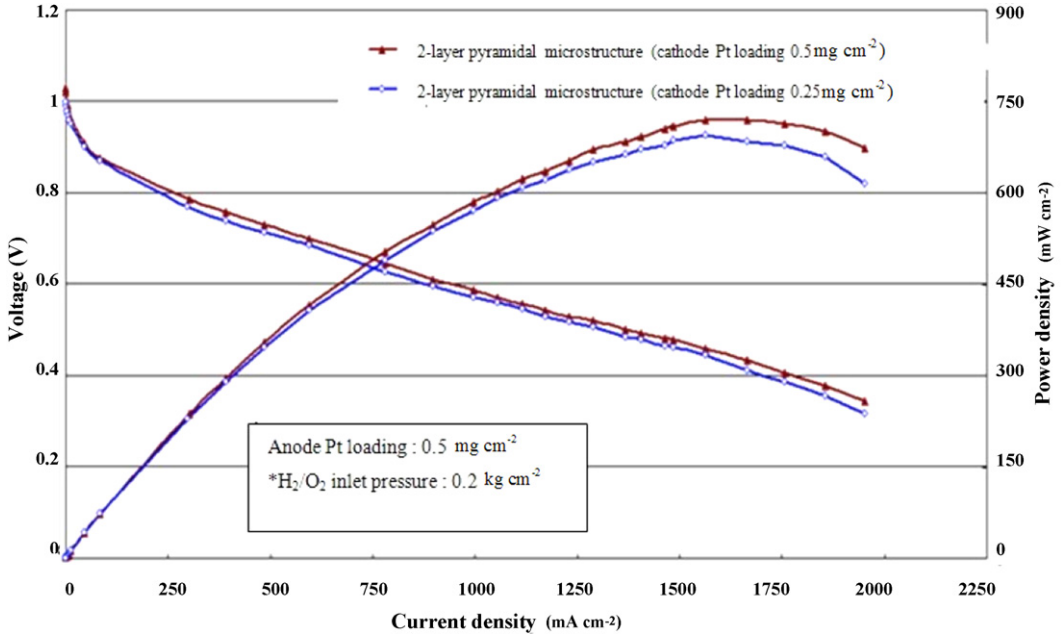

Fig. 10. Performance comparison with Pt loading of the cathode cut in half.

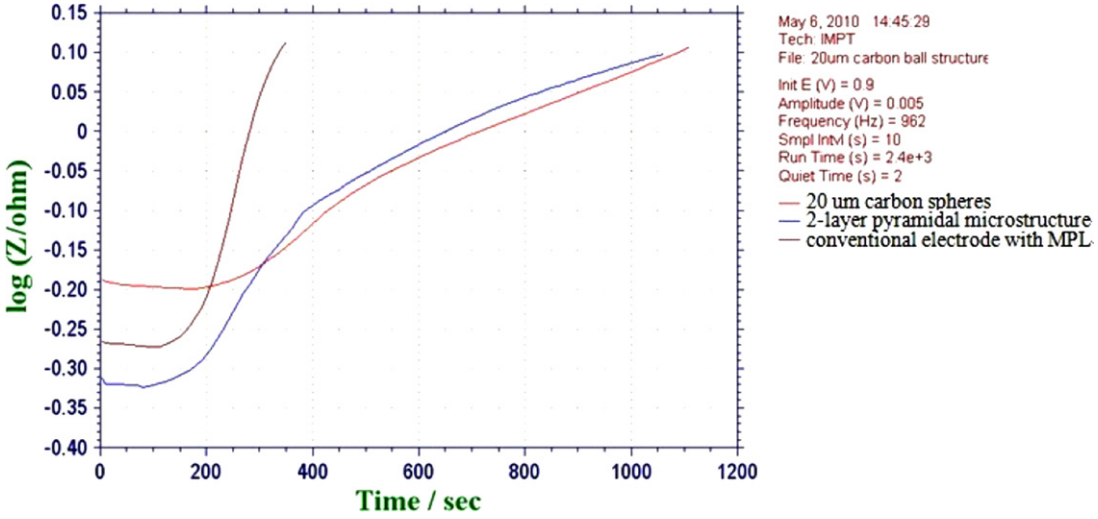

Fig. 11. Impedance of an MEA during drying.

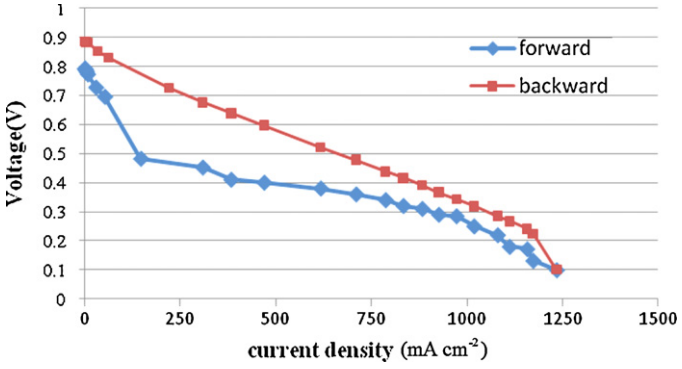

Fig. 12. Performance of the 1st cycle of an MEA with a 2-layer-pyramidal-microstructure cathode using the periodic linear sweep method.

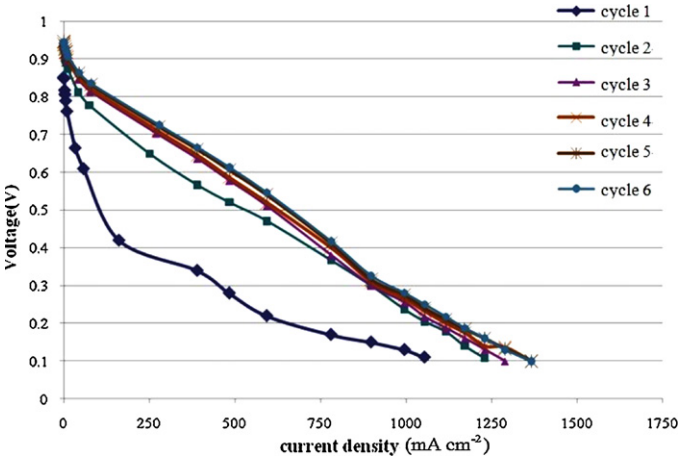

Fig. 14. Performance of an MEA with a conventional structure (with flat CL and MPL) in periodic linear sweep tests (forward-test results only).

that only the membrane initially has water for all the MEAs under testing.

Fig. 12 demonstrates typical behaviour in the first cycle: Forward cycle performance is very poor since it begins with a dry MEA, followed by significant improvement on the backward cycle because the needed water is being continuously produced. The performance improves with running time and number of cycles until steady state is reached where the responses of forward and backward cycles nearly coincide, as shown in Fig. 13. Fig. 14 shows the multiple cyclic performance test results of a conventional structured MEA (with a flat catalyst layer and MPL). For clarity, only the forward half cycles are plotted. It barely changes and approaches steady state after the third cycle. The reduction in ohmic overpotential is certainly a direct result of the produced water, but the significant improvement over the entire current spectrum indicates that it is mainly due to the increase in reaction sites.

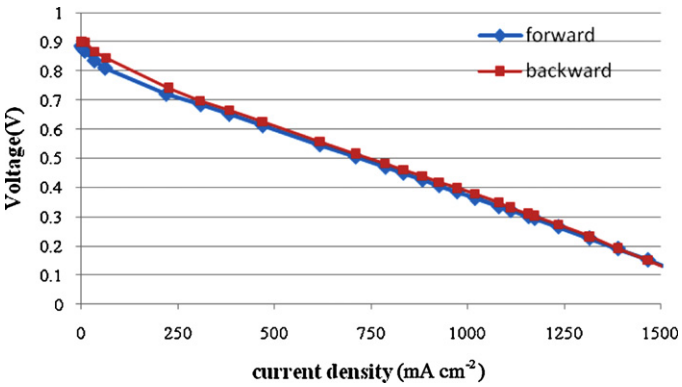

Fig. 13. Performance of the 4th cycle of an MEA with 2-layer-pyramidal-microstructure cathode using the periodic linear sweep method.

Fig. 15 shows the multiple cyclic performance test results of an MEA with a 2-layer-pyramidal-microstructured catalyst layer. There is a "jump" in performance between the 3rd and 4th cycles as it is approaching the steady state. This phenomenon appears in all MEAs with microstructures, but not in conventionally structured ones.

3.3. Proposition on the development of water and major reaction sites

As illustrated in Fig. 16, for a typical pore inside the catalyst layer, the electrochemical reaction begins near the membrane due to the initial drying process. The continuous water film on the pore wall is gradually established (perhaps with the help of Nafion) starting from the membrane and expanding outward toward the MPL

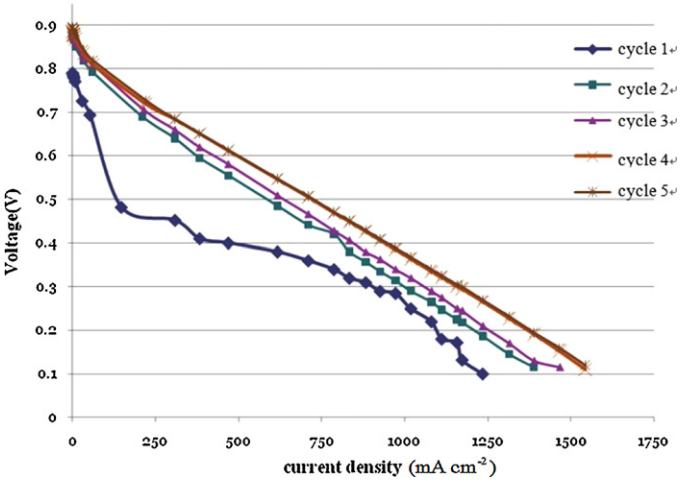

Fig. 15. Performance of a MEA with 2-layer-pyramidal-microstructure cathode in the periodical linear sweep tests (forward-test results only).

as produced vapour diffuses. Protons may be transported to any place where this water film extends. As more reaction sites are created (satisfying the triple phase boundary (TPB) condition) more vapour will be produced, thus increasing the area of the water film. The inner portion (membrane side) of the pore will have a smaller supply of oxygen or electrons if the number of reaction sites or the area of the water film is more than what is needed to meet the current demand. As a result, the major reaction sites (MRS) move slowly away from the membrane. Vapour diffuses in all directions and condenses at places where temperature is lower, i.e., at both ends of the pore. Accumulated condensed water may block the narrower part of the pore. If it is to the MPL side and outside the reach of the water film, the reaction will be diminished due to reduced oxygen supply and will resume operation when the blockage is removed through evaporation. But if the blockage is within the extension of the water film, since the proton can be transported beyond the blocked point, the MRS will shift entirely above it and the inner portion will remain blocked and, thus, a water "surface" emerges. The aforementioned processes will be repeated and this "surface" moves outward gradually until it reaches the last section of the pore where the amount of vapour produced by the MRS can be removed completely by the MPL and the rest of the system.

Ideally, all pores inside the catalyst layer can pass, although tortuously, from the membrane to the MPL and then farther into the carbon cloth/paper. They may have branches and many close interconnections among themselves. However, these will not significantly alter the development of the water surface described above, since all the pores are functioning at the same time and at pretty much the same pace, and the exchange of oxygen and vapour among them is limited and will not change the general trend unless some of the branches are responsible for mass transport only. Therefore, the movement of the water surface may be described as seen in Fig. 17.

Here we propose a "theory" on the development of water and major reaction sites inside the catalyst layer of the cathode of a PEMFC: There is a general water "surface" inside the catalyst layer. It is not necessarily flat. Major electrochemical reactions can only occur above this surface (on the MPL side) and within a limited height. As more water is produced, the surface will "move" from the membrane toward the MPL. The vapor generation rate (current load) relative to the vapor removal rate of the rest of the cell components will determine the steady state position (or the existence) of this water surface.

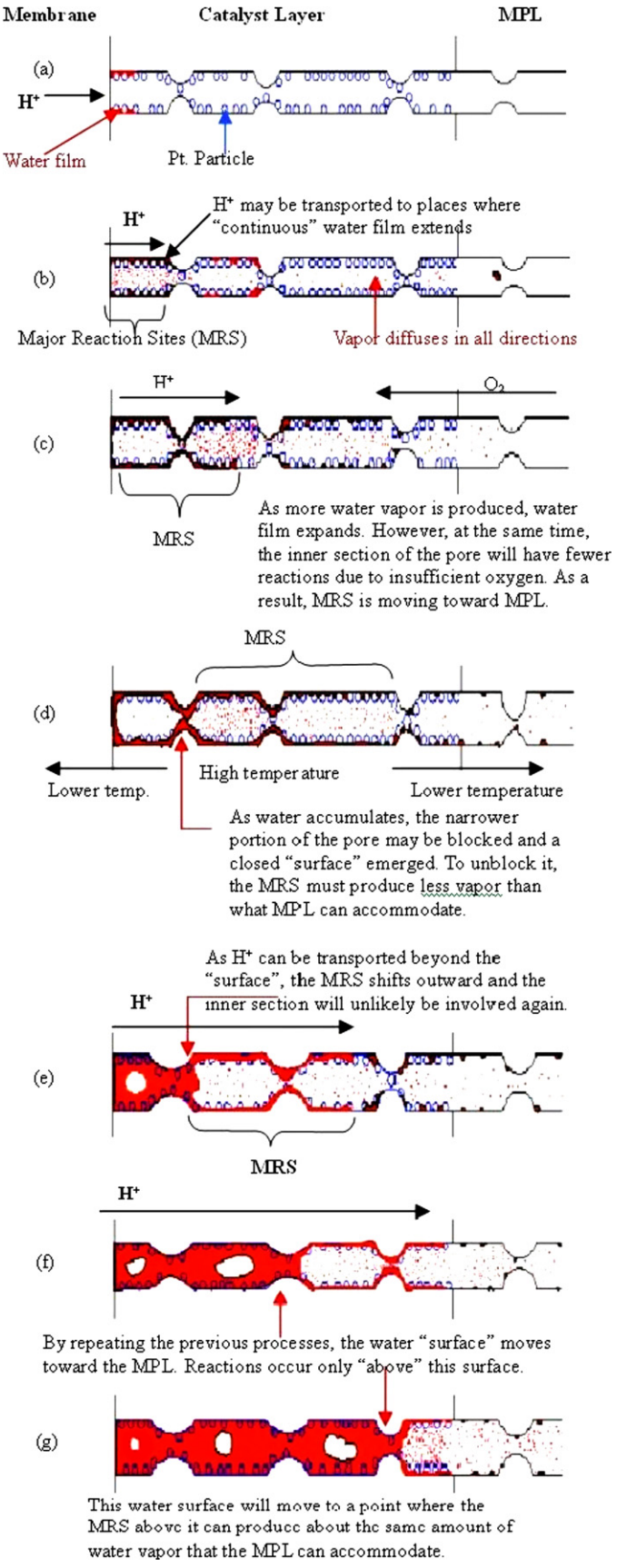

Fig. 16. Proposition on the development of water and major reaction sites in a reacting pore inside the catalyst layer.

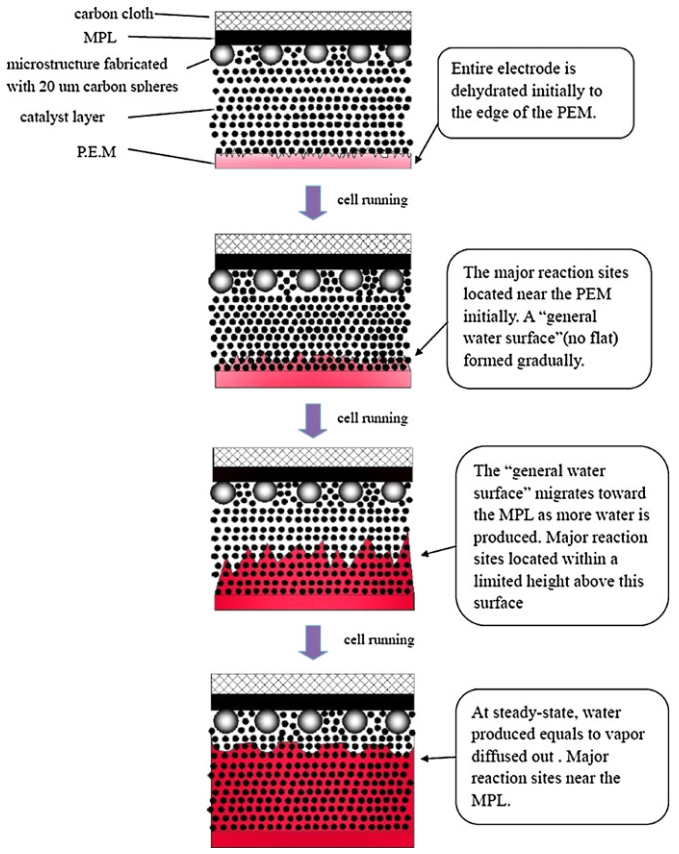

Fig. 17. Proposition on the development of water "surface" inside the catalyst layer. Large spheres represent microstructures.

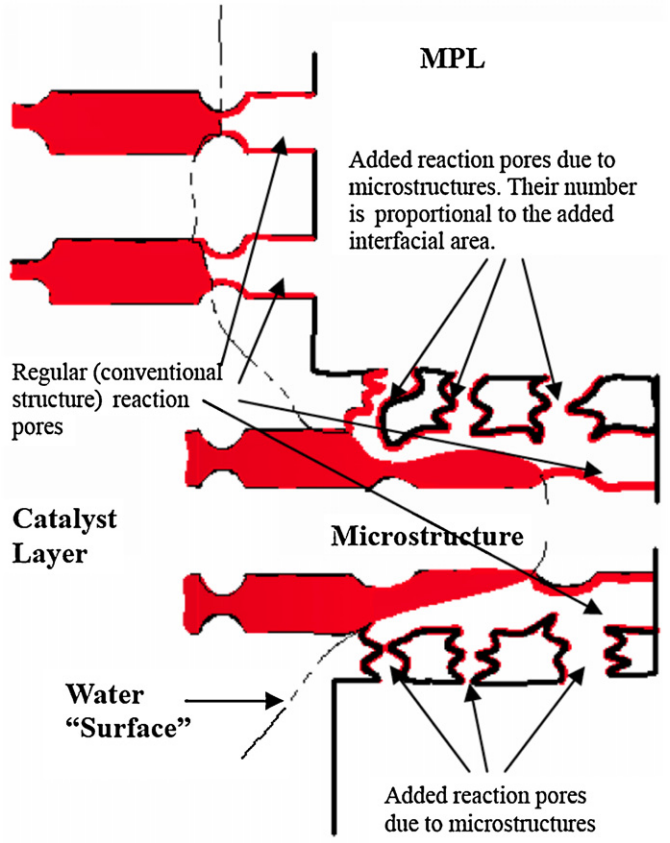

Fig. 18. Microstructure creates more reacting pores in a short duration as it approaches the water "surface".

3.4. How microstructures work

For a conventional electrode with a flat catalyst layer, the total area of the MRS reaches steady state quite early, even though the MRS is still "moving" toward the MPL, and the response changes little after the second cycle as shown in Fig. 14. However, for the cathode with microstructures, when this "water surface" reaches the area of a microstructure, a large number of "additional" reacting pores (with openings on the extra interface area created by the microstructure) will be brought into action within a short period of time, as shown in Fig. 18. As a result, a performance "jump" appears at the fourth cycle, as shown in Fig. 15. The number of these "additional" reacting pores is exactly proportional to the increase in interface area of the CL and the MPL (with uniform spherical carbon support, the number of pores is directly proportional to the size of the area) and this explains the correlativity between area and performance. In addition, the fact that the steady-state performance improves across the entire current spectrum (see Figs. 6–9) also indicates that the improvement comes mainly from the decrease in activation overpotential through the increase in exchange current density due to added reaction sites.

To summarize, this proposition can satisfactorily explain our experimental observations (1) microstructures of various dimensions, quantities, heights, and shapes provide a 20–60% increase in the interface area and produce the same percentage of increase in performance; (2) the cathode's Pt loading was reduced from 1 mg cm^{-2} to 0.5 mg cm^{-2}, and then again to 0.25 mg cm^{-2} with the cell suffering no significant performance loss; (3) in the periodic linear sweep tests, all cathodes with microstructures showed an obvious "jump" in performance when approaching steady state, but no such "jump" occurred for electrodes with a conventional flat-CL design.

4. Conclusions

Microstructures fabricated on the interface of the catalyst layer and the micro porous layer can very effectively enhance an electrode's performance and the extent of this improvement is directly indicated by the size of the interface area added due to structural modification. This increased effectiveness may be explained by a theory on the movement of water inside the catalyst layer proposed as follows:

There is a general water "surface" inside the CL. It is not necessarily flat. Major electrochemical reactions occur above this surface (on the MPL side) and within a limited height. As more water is produced, the surface will "move" from the membrane toward the MPL. The vapor generation rate (current load) relative to the vapor removal rate of the rest of the cell components will determine the steady state position (or the existence) of this water surface.

Many factors affect the position of this water surface. A detailed understanding of how water is developed in the catalyst layer will help in the future design and operation of electrodes.

Acknowledgements

The authors wish to thank the National Science Council of Taiwan, Republic of China, for its financial support of this work through the Grant no. NSC 96-2221-E-110-026-MY3.

References

[1] M.-S. Lee, L.-J. Chen, T.-H. Chen, J. Fuel Cell Sci. Technol.: Trans. ASME 6 (February) (2009) 011006.

[2] S.A. Cho, E.A. Cho, I.-H. Oh, H.-J. Kim, H.Y. Ha, S.-A. Hong, J.B. Ju, J. Power Sources 155 (2006) 286–290.
[3] M. Prasanna, E.A. Cho, H.-J. Kim, T.-H. Lim, I.-H. Oh, S.-A. Hong, J. Power Sources 160 (2006) 90–96.
[4] M. Hakan Yildirim, J. te Braake, H. Can Aran, D.F. Stamatialis, M. Wessling, J. Membr. Sci. 349 (2010) 231–236.
[5] Y. Zhang, J. Lu, S. Shimano, H. Zhou, R. Maeda, Electrochem. Commun. 9 (6) (2007) 1365.
[6] A.D. Taylor, E.Y. Kim, V.P. Humes, J. Kizuka, L.T. Thompson, J. Power Sources 171 (2007) 101–106.
[7] H.-N. Su, Q. Zeng, S.-J. Liao, Y.-N. Wu, Int. J. Hydrogen Energy 35 (2010) 10430–10436.
[8] M. Srinivasarao, D. Bhattacharyya, R. Rengaswamy, S. Narasimhan, Int. J. Hydrogen Energy 35 (2010) 6356–6365.
[9] Y.-G. Yoon, T.-H. Yang, G.-G. Park, W.-Y. Lee, C.-S. Kim, J. Power Sources 118 (2003) 189–192.
[10] K.-H. Kim, H.-J. Kim, K.-Y. Lee, J.H. Jang, S.-Y. Lee, E. Cho, I.-H. Oh, T.-H. Lim, Int. J. Hydrogen Energy 33 (2008) 2783–2789.
[11] A. Bazylak, Int. J. Hydrogen Energy 34 (2009) 3845–3857.
[12] J. St-Pierre, J. Electrochem. Soc. 154 (7) (2007) B724–B731.
[13] S. Tsushima, K. Teranishi, S. Hirai, Electrochem. Solid State Lett. 7 (9) (2004) A269–A272.
[14] R. Satija, D. Jacobson, M. Arif, S. Werner, J. Power Sources 129 (2004) 238–245.
[15] C. Hartnig, I. Manke, R. Kuhn, S. Kleinau, J. Goebbels, J. Banhart, J. Power Sources 188 (2009) 468–474.
[16] S.J. Lee, N.-Y. Lim, S. Kim, G.-G. Park, C.-S. Kim, J. Power Sources 185 (2008) 867–870.
[17] P. Sinha, P. Halleck, C.-Y. Wang, Electrochem. Solid State Lett. 9 (7) (2006) A244–A248.
[18] X. Yang, F. Zhang, A. Lubavy, C.Y. Wang, Electrochem. Solid State Lett. 7 (11) (2004) A408–A411.
[19] K. Tuber, D. Pocza, C. Hebling, J. Power Sources 124 (2003) 403–414.
[20] A. Bazylak, D. Sinton, Z.-S. Liu, N. Djilali, J. Power Sources 163 (2007) 784–792.
[21] S. Litster, D. Sinton, N. Djilali, J. Power Sources 154 (2006) 95–105.
[22] C. Hartnig, I. Manke, R. Kuhn, N. Kardjilov, J. Banhart, W. Lehnert, Appl. Phys. Lett. 92 (2008) 134106-1–134106-3.
[23] F.-Y. Zhang, D. Spernjak, A.K. Prasad, S.G. Advani, J. Electrochem. Soc. 154 (11) (2007) B1152–B1157.
[24] A.Z. Weber, M.A. Hickner, Electrochim. Acta 53 (2008) 7668–7674.
[25] J.H. Nam, M. Kaviany, J. Heat Mass Transfer 46 (2003) 4595–4611.
[26] L. Hao, H. Yu, J. Hou, W. Song, Z. Shao, B. Yi, J. Power Sources 177 (2008) 404–411.